

# Comparing the impact of different thermal comfort constraints on a model-assisted control design process

E.G. Kontogianni<sup>#1</sup>, G.I. Giannakis<sup>#2</sup>, G.D. Kontes<sup>#3</sup>, D.V. Rovas<sup>#4</sup>

<sup>#</sup>*Department of Production Engineering and Management,  
Technical University of Crete, Chania, Greece*

<sup>1</sup>ekontogianni@isc.tuc.gr

<sup>2</sup>ggiannakis@isc.tuc.gr

<sup>3</sup>gkontes@isc.tuc.gr

<sup>4</sup>rovas@dpem.tuc.gr

## Abstract

*In the design of supervisory controllers for managing energy in buildings, model-based control design approaches have recently attracted significant attention. The control-design problem in these cases is typically posed as a constrained minimization problem: given a simulation model acting as a surrogate of the building, identify a controller that minimizes a cost function, say energy, subject to the constraint that thermal comfort stays within acceptable levels. The use of a thermal comfort model can be the means for estimating comfort so that the mathematical programming problem can be formulated. In the present paper, we investigate how the choice of thermal comfort model affects the quality of the resulting controller. We consider a building simulated in EnergyPlus and design, under the same conditions, controllers using three different thermal comfort models: the model of Fanger, the two-node Pierce model, and the KSU two-node model. A comparative study is performed to draw conclusions upon the effects that this selection has with respect to the performance of the resulting controller.*

**Keywords – thermal comfort; BEMS; GenOpt; Control Design**

## 1. Introduction

In the design of supervisory controllers for managing energy in buildings, model-based control design approaches have recently attracted significant attention. The control-design problem in these cases is typically posed as a constrained minimization problem: given a simulation model acting as a surrogate of the building, identify a controller that minimizes a cost function, say energy, subject to the constraint that thermal comfort stays within acceptable levels. All model-based control design approaches require some notion of thermal comfort: from simple temperature-tracking [15], [16] to the use of more elaborate indices [4], [9], [13]. As can be expected, the methodology selected to model thermal comfort will have an effect to the resulting controller.

In the present paper, three widely-used models, the Fanger [7], Pierce [8] and KSU [2] are selected. A comparative study demonstrating the effect

of each of the above three complex comfort indices in BEMS design is performed. A detailed thermal model in EnergyPlus of an office building is available and using the Generic Optimization Program (GenOpt) [17], a control design optimization problem, attempting to balance the tradeoff between energy consumption and user comfort levels is solved for one selected day and for different comfort values for all indices.

## 2. Methodology

The overall methodology towards evaluating the effect of the different indices is based on the availability of a simulation model assimilating the building thermal behavior. This model should be able to evaluate the energy consumption evoked by any control strategy, along with the respective thermal comfort indices. Having such a model at hand, allows defining a constrained optimization problem, in which an optimization algorithm is required to adjust the tunable parameters of a control function, to minimize energy consumption and preserve thermal comfort for the occupants.

### A. Controller

To start, the parametric controller used to populate the control decisions on the building is defined as a linear function, transforming a set of inputs (such as temperature, humidity, etc.) to control decisions as follows:

$$u_t = \theta \times x_t. \quad (1)$$

Here,  $t$  is the time index,  $u_t$  are the control actions at time  $t$ ,  $x_t$  are the states at time  $t$  and  $\theta$  is a set of weights consisting the controller. It is obvious, that the problem of producing efficient control actions is transformed to the one of selecting proper weights  $\theta$ .

### B. Optimization Problem

To produce efficient control strategies, the values of the control weights  $\theta$  from (1) have to be optimized with respect to a proper performance index. Since in our case we are interested in energy-efficient control strategies that preserve thermal comfort, the optimization problem has the following form:

$$\begin{aligned} & \min \sum_{t=1}^T E_t, \\ & s. t. \left( \frac{1}{T} \sum_{t=1}^T C_t^i \right) < C_l^i, \quad \forall i \in \{1, 2, \dots, N\}. \end{aligned} \quad (2)$$

Here,  $t$  is the time-index,  $T$  is the time-period we are interested in optimizing the controller,  $E_t$  is the energy consumption in the interval  $[t - 1, t]$ ,  $C_t^i$  is the value of the thermal comfort constraint at time  $t$  for room  $i$ ,  $C_l^i$  an upper discomfort bound for room  $i$  and  $N$  the number of rooms. Therefore, we define a problem where the goal is to minimize the total energy consumption

for a period of time  $T$ , say one day, requiring the average value of a thermal comfort index to remain below a predefined upper limit in that period.

### C. GenOpt

To solve the optimization problem GenOpt was used [17]. GenOpt is an optimization software package written in Java and developed by Lawrence Berkeley National Laboratory, providing a large variety of optimization algorithms for the task and being able to integrate with external simulation software. Since the performance evaluation of each controller parameter set is performed by the building thermal simulation model, defined by external thermal simulation software, consecutive *parallel* calls on the model are performed as shown in Fig. 1. Initially, a set of candidate control parameters is created by the algorithm and each parameter set is assigned to a dedicated simulation execution thread. The performance (energy consumption and comfort levels) of each set is evaluated on the simulator, communicated back to GenOpt and the whole process is repeated until convergence.

GenOpt, although allows definition of any constraint optimization problem, facilitates different representation for the problem than in (2), using penalty functions:

$$\min \left( \sum_{t=1}^T E_t + m \sum_{i=1}^N \max(0, g^i) \right), \text{ with} \quad (3)$$

$$g^i = \left( \frac{1}{T} \sum_{t=1}^T C_t^i - C_i^i \right)^2.$$

Here, the symbols are the same as in (2) and the optimization problem is equivalent, but the weight  $m$  is used to adjust the trade-off between energy consumption and thermal comfort levels.

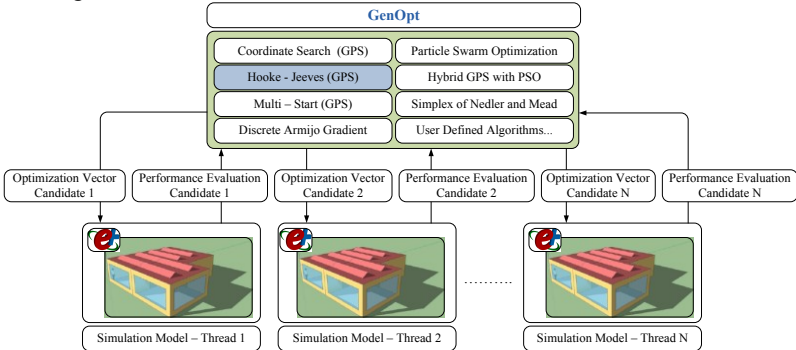


Fig. 1 GenOpt-EnergyPlus interaction

#### *D. Simulation Model*

To solve the optimization problem, a multitude of values of the control weights  $\theta$  from (1) has to be evaluated on the simulation model, which should be able to calculate the energy consumption and the thermal comfort levels for each controller. Although a plethora of building thermal simulation software would be suitable for the task, in the present work EnergyPlus [5] simulation engine is used. As part of a simulation using EnergyPlus five widely-used thermal comfort indices can be calculated: Fanger, Pierce, KSU, the Adaptive Comfort Model based on ASHRAE Standard 55-2010 [1] and Adaptive Comfort Model Based on the European Standard EN15251-2007 [3]. As stated earlier, here, the effects of the first three of these models are investigated, whose main idea is to predict the thermal sensation of people using a seven- or nine-point sensation scale (see Fig. 2).

These three models apply an energy balance to the human body and use the energy exchange mechanisms along with physiological models to predict the thermal sensation. However, they differ on the physiological models that are used to evaluate the heat transfer through and from the body and the neural control of shivering, sweating and skin blood flow.

With respect to the Pierce model [8], the human body is represented by a cylinder that consists of an inner cylinder named core and an outer one that corresponds to the skin shell. In this way, three different temperatures are defined; the skin shell temperature, the core compartment temperature and the mean body temperature; these temperatures along with the skin wettedness and the rate of heat exchange between the skin and environment, are used for the calculation of the effective temperature. Thus, the Pierce model estimates the heat transfer between the core and the skin. On the contrary, the Fanger model does not assume something correlated, but implements calculations using physical and thermal data.

The Fanger model [7], as well as the Pierce model, subtract the heat losses from the internal heat production rate of an occupant per unit area. Therefore, these models estimate respiratory heat loss, radiant and convective heat loss from the body surface and evaporative heat loss from the skin. Apart from respiratory heat loss, differentiates how the other terms of heat loss are calculated. Both models use radiant temperature, ambient temperature, skin temperature, barometric pressure and estimate other factors, such as convection heat transfer coefficient and clothed body surface temperature, in completely different way, in order to perform thermal comfort calculations. This is an additional difference that can give an explanation to the extremely different behavior of the two models. Predicted Mean Vote (PMV) (see Fig. 2) and Predicted Percentage of Dissatisfied people (PPD) in Fanger model, and PMV Effective Temperature (PMVET) (see Fig. 2), PMV Standard Effective Temperature (PMVSET), Predicted Discomfort Vote (DISC) and Thermal Sensation Vote (TSENS) in Pierce model, are used to quantify the thermal comfort.

The KSU model [2] is based on the Pierce model concept, having the difference of calculation between cold and warm environments. The index that occurs is known as Thermal Sensation Vote (TSV). In warm environments where the present application is performed, KSU is based on changes in the skin wettedness and TSV index is calculated through relative humidity and the ratio between skin wettedness due to regulatory sweating and skin wettedness at thermal neutrality.

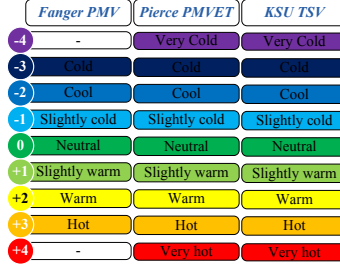


Fig. 2 Seven and nine point thermal sensation scales

### 3. Application

To investigate the effect of thermal comfort index selection in control design, the thermal simulation model of a sample office building, located in Athens, Greece, is modeled using EnergyPlus (Fig. 3). The building comprises three office rooms, with large surface windows and an Ideal Load A/C unit installed on each of them. Each room is defined as a separate thermal zone [13].

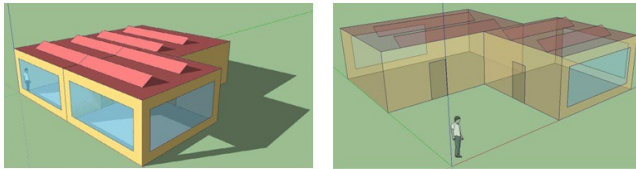


Fig. 3 Geometry of the sample building created in OpenStudio plugin for Google SketchUp

Each actuating component of the building is controlled by a linear controller, as in (1). Every 10 minutes, a vector of states for each room of the building, containing the outside temperature, outside humidity ratio, global solar radiation, wind speed, wind direction, room temperature, room humidity ratio and a binary value indicating if the room is occupied (with one for occupied) is mapped (through the weights  $\theta$ ) to the control vector, which consists of each room's thermostat cooling setpoint and window opening angle – these two are the controllable parameters.

A set of optimization tasks is defined for each thermal comfort index, containing different upper bound values for the constraint  $C_i^j$  in (3), which

based on the ISO 7730 [11] recommendations according to Fanger, shown in Table 1. Note here that the same constraint values are used for Pierce and KSU.

Table 1 Categories of thermal environment according to ISO 7730 [11]

Category	Absolute Value of Fanger Predicted Mean Vote (AbsPMV)
A	AbsPMV<0.2
B	AbsPMV<0.5
C	AbsPMV<0.7

Since each optimization task consists of a constraint and continuous optimization parameters ( $\theta$ ), Hooke-Jeeves is the selected optimization algorithm [17], in accordance to GenOpt guidelines, which is a local search algorithm of the Generalized Pattern Search Algorithms family. Here, an initial solution (a parameter vector  $\theta$  from (1)) is provided to the algorithm. Subsequently, a constant value ( $\Delta\theta$ ) is added and subtracted sequentially from each of the initial parameters. The parameter variations that improve the cost function value are stored to a temporary parameter vector, based on which and on algorithm parameters, a map containing candidate solutions over the parameter space is constructed. Each value of this map is investigated similarly as previously. If constructing the map is not possible, due to absence of any solutions that improve the objective function, a detailed local search process is initiated around the solution with the best cost function value. If this new local search also fails, the whole process re-initiates using the next value of constructed map, but with  $\Delta\theta$  reduced. Finally, the optimization process terminates if a maximum number of iterations has exceeded or a fixed number of iterations has concluded to the same solution, or the maximum number of  $\Delta\theta$  reductions has been reached.

#### 4. Experiments – Results

Moving to the experimental setup, August 3<sup>rd</sup> appears to be the warmest day according to Athens weather file, with maximum outdoor dry bulb temperature at 36.2°C, thus is selected as our test day. On the other hand, the actual simulation starting time is July 27<sup>th</sup>, in order to assimilate the initial conditions of the building at the beginning of August 3<sup>rd</sup> (warming-up phase). During these seven warming-up days, the thermostat setpoints of the A/C units are set to 25 °C and the windows are closed, when the building is occupied, otherwise the setpoints are set to 50°C (i.e. the HVAC is switched-off) and the windows are opened. This same rule-based controller is also simulated once for the day of interest, in order to collect state-action vectors and design an initial controller (initial values for the weights  $\theta$ ), by solving the resulting system of equations of (1).

Fig. 4, Fig. 6 and Fig. 8 represent the reliance of energy consumption to thermal comfort constraint. The axes of thermal comfort show the average

thermal comfort indices of the three zones and the energy consumption axes show the average energy consumption of the three zones. The first batch of optimization tasks use the Fanger PMV index, is shown in Fig. 4. Here, the PMV appears to be less strict than the other two, allowing the optimization process to produce controllers that are able to satisfy even stringent discomfort constraints (see Table 1). This behavior can be explained through the estimation of the convection heat transfer coefficient in the PMV; the aggregation of clothed body surface temperature and ambient temperature lead to low values of PMV index for low thermostat set-points. Thus, compared to the other two thermal comfort indices, Fanger PMV index requires the least amounts of energy, for the lowest comfort constraint values. Moving on, the results of the optimization tasks using Pierce PMVET index are shown in Fig. 7. PMVET appears to be unfitting for the task, since it leads the optimization process to controllers that excessively cool the rooms. In fact, for the lowest comfort bound (0.2), the optimization algorithm is unable to produce a proper control strategy that satisfies the constraint. In this case, the lowest achieved PMVET comfort value is 0.456, corresponding to a low PMV value (-0.6), indicating cold-induced discomfort in the rooms. In fact, a closer look at the resulting control strategy reveals that all A/C units are set to 20°C for all occupancy hours, rendering the resulting controller unsuitable for the task (Fig. 7). This behavior is caused by the overestimation of skin temperature and the underestimation of skin wettedness in Pierce model calculations.

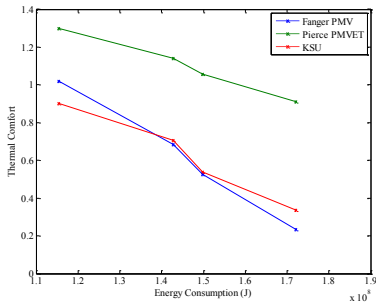


Fig. 4 Performance evaluation setting as constraint the Fanger PMV

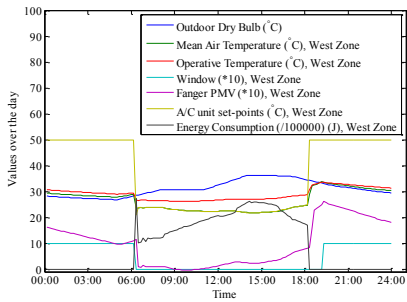


Fig. 5 Optimized controller-west zone, setting as constraint AbsPMV=0.2

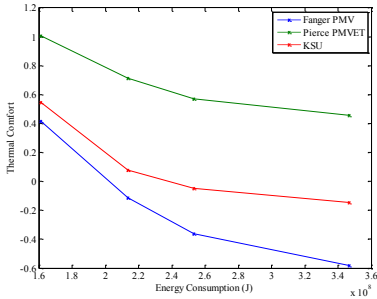


Fig. 6 Performance evaluation setting as constraint the Pierce PMVET

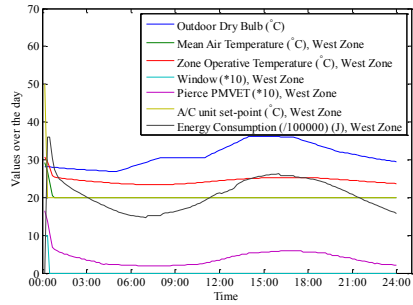


Fig. 7 Optimized controller-west zone, setting as constraint AbsPMVET=0.2

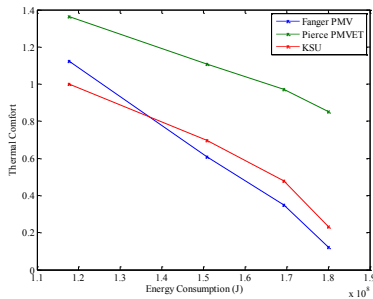


Fig. 8 Performance evaluation setting as constraint the Ksu TSV

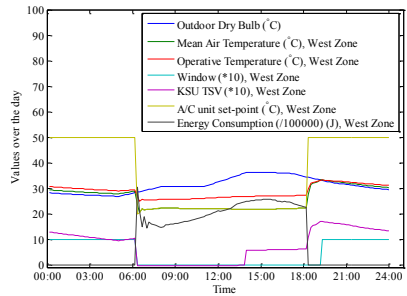


Fig. 9 Optimized controller-west zone, setting as constraint AbsTSV=0.2

Finally designs using the KSU index are presented in Fig. 6, where it becomes apparent that even though KSU is based on Pierce model calculations, the behavior differs significantly. This difference stems from the details of KSU model calculations, which follow the same reasoning as Pierce model for cold environments, but follow a different path with respect to the skin wettedness calculations for warm environments. In general, KSU and Fanger PMV indices trends are similar.

With respect to the optimized controller, Fig. 5, Fig. 7 and Fig. 9 show indicatively the behavior of each index to the controller actions during the simulation day. Here the upper limit of the constraint was set to 0.2. The controller based on Fanger PMV index (Fig. 5), varies smoothly at [21, 24] °C. Due to low outdoor dry bulb temperature until 11:00, the index levels get very close to 0 (neutral), consuming the lower amounts of energy compared with the energy consumption of the rest day. After this period, the required energy as well as the index values increase, due to high outdoor dry-bulb temperature. As previously referred, the optimization with Pierce PMVET fails to reach the bound of 0.2, although the thermostat temperature is set on the lowest allowed setpoint of the A/C unit (20 °C). Regarding the KSU TSV



index, temperature setpoint has similar trends compared to Fanger, varying at [20, 23] °C.

## 5. Conclusion

In the present work, a Generalized Pattern Search Algorithm was used to find solutions that satisfy thermal comfort acceptable limits and minimize the required energy consumption. The optimization constraints, consist of the thermal comfort levels, set according to ISO 7730 categories for thermal environment. Hence the impact of Fanger PMV, Pierce PMVET and KSU TSV estimated by EnergyPlus software, to the control design process was analyzed. Fanger PMV index, is proved to be the most sensitive and relax to the A/C unit setpoint changes and it can reach with no large amounts of energy, to low levels. Pierce PMVET seems to be preserved in higher levers despite the low thermostat temperatures. KSU TSV index has similar trends with Pierce PMVET regarding sensitivity, but it can easily reduce its levels for values close to 1.

## 6. Acknowledgment

The research leading to these results has been partially funded by the European Commission FP7-ICT-2007-9.6.3, Energy Efficiency under contract #248537 (PEBBLE) and European Commission FP7-ICT-2011-6, ICT Systems for Energy Efficiency under contract #288409 (BaaS).

## 7. References

- [1] ASHRAE. Standard 55-2010 - Thermal Environmental Conditions for Human Occupancy (ANSI approved). American Society of Heating, Refrigerating and Air Conditioning Engineers, Atlanta, GA, 2010.
- [2] N.Z. Azer and S. Hsu. The prediction of Thermal Sensation from Simple model of Human Physiological Regulatory Response. ASHRAE Transactions, 83( 1), 1977.
- [3] CEN. Standard EN15251 Indoor environmental input parameters for design and assessment of energy performance of buildings addressing indoor air quality, thermal environment, lighting and acoustics. Bruxelles, European committee for Standardisation, 2007.
- [4] J. Cigler, S. Privara, Z. Vaňa, E. Žáčková and L. Ferkl. Optimization of predicted mean vote index within model predictive control framework: Computationally tractable solution. Energy and Buildings, 52: 39-49, 2012.
- [5] D.B. Crawley et al. EnergyPlus: creating a new-generation building energy simulation program. Energy and Buildings, 319-331, 2001.
- [6] T.J. Doherty and E.A. Arens. Evaluation of the physiological bases of thermal comfort models. ASHRAE Transactions, 94(15), 1988.
- [7] P.O. Fanger. Thermal Comfort-Analysis and Applications in Environmental Engineering. Danish Technical Press, Copenhagen, 1970.
- [8] A.P. Gagge, J.A. Stolwijk and Y. Nishi. An Effective Temperature Scale Based on a Simple Model of Human Physiological Regulatory Response. ASHRAE Transactions, 70(1), 1970.

- [9] G.I. Giannakis, G.D. Kontes, E.B Kosmatopoulos, and D.V Rovas. A model-assisted adaptive controller fine-tuning methodology for efficient energy use in buildings. In Mediterranean Conference on Control & Automation, 49 –54, 2011.
- [10] T. Haase, A. Hoh, P. Matthes and D. Muller. Integrated simulation of building structure and building services installations with Modelica. Proceedings of Roomvent, 2007.
- [11] International Organization for Standardization. ISO7730:2005: Ergonomics of the thermal environment - Analytical determination and interpretation of thermal comfort using calculation of the PMV and PPD indices and local thermal comfort criteria. International Organization for Standardization, Geneva, Switzerland, 2005.
- [12] S.A. Klein, W.A. Beckman and J.A. Duffie. TRNSYS - A TRANSIENT SIMULATION PROGRAM. ASHRAE Transactions, 82 : 623-633, 1976.
- [13] G.D. Kontes, G.I. Giannakis, E.B. Kosmatopoulos and D.V. Rovas. Adaptive Fine-Tuning of Building Energy Management Systems Using Co-Simulation. IEEE Multi-Conference on Systems and Control, 2012.
- [14] G.D. Kontes, G.I. Giannakis, G.N. Lilis, E.B. Kosmatopoulos, and D.V. Rovas. PEBBLE BO&C System. PEBBLE Deliverable 3.2, 2011.
- [15] Y. Ma, F. Borrelli, B. Hancey, B. Coffey, S. Bengesa and P. Haves. Model predictive control for the operation of building cooling systems. American Control Conference (ACC), 5106-5111, 2010.
- [16] F. Oldewurtel, A. Parisio, C.N. Jones, D. Gyalistras, M. Gwerder, V. Stauch, B. Lehmann and M. Morari. Use of model predictive control and weather forecasts for energy efficient building climate control. Energy and Buildings, 45:15-27, 2012.
- [17] M. Wetter. GenOpt, Generic Optimization Program, User manual Version 3.1.0. Simulation Research Group, Building Technologies Department, Environmental Energy Technologies Division, Lawrence Berkeley National Laboratory, Berkeley, CA 94720.